


# A Novel Tri-Layer Cellulose-Based Membrane for the Capture and Analysis of Mainstream Smoke of Tobacco

Xuyan Song <sup>1</sup>, Min Wei <sup>1,\*</sup>, Yunlu He <sup>1</sup>, Xi Pan <sup>1</sup>, Xinjiao Cui <sup>2</sup>, Xiaodi Du <sup>2,\*</sup> and Junsheng Li <sup>2,\*</sup> 

<sup>1</sup> Technology Centre of Hubei China Tobacco Industry Co., Ltd., Wuhan 430051, China; songxy@hbtobacco.cn (X.S.); heyunlu@hbtobacco.cn (Y.H.); 11013210@hbtobacco.cn (X.P.)

<sup>2</sup> School of Chemistry, Chemical Engineering and Life Sciences, Wuhan University of Technology, Wuhan 430070, China; 304805@whut.edu.cn

\* Correspondence: weimin@hbtobacco.cn (M.W.); duxiaodi@msn.com (X.D.); li\_j@whut.edu.cn (J.L.)

**Abstract:** Efficient capture of particulate matter in the smoke mainstream using low-cost filter pads is important for cost-effective analysis of mainstream smoke. The Cambridge filter pad (CFP) is the standard material for the collection of particulate matter in the mainstream. In this work, we report a low-cost alternative to CFP, which is composed of a cellulose acetate fiber (CAF) interlayer and two cotton fiber (CF) layers on both sides. The CF/CAF/CF filter exhibited high affinity toward typical tobacco additives such as glycerol and glycerol triacetate. In addition, the CF/CAF/CF filter had a favorable porous structure for the trapping of particulate matter. Due to these beneficial features, the CF/CAF/CF filter exhibited improved particulate matter trapping performance. These results suggest that the as-developed CF/CAF/CF filter could be a low-cost alternative to CFP.

**Keywords:** cellulose; cellulose acetate; porous structure; tobacco; trapping; particulate matter; mainstream smoke



**Citation:** Song, X.; Wei, M.; He, Y.; Pan, X.; Cui, X.; Du, X.; Li, J. A Novel Tri-Layer Cellulose-Based Membrane for the Capture and Analysis of Mainstream Smoke of Tobacco. *Appl. Sci.* **2022**, *12*, 4196. <https://doi.org/10.3390/10.3390/app12094196>

Academic Editors: Elza Bontempi and Giorgia Spigno

Received: 1 March 2022

Accepted: 11 April 2022

Published: 21 April 2022

**Publisher's Note:** MDPI stays neutral with regard to jurisdictional claims in published maps and institutional affiliations.



**Copyright:** © 2022 by the authors. Licensee MDPI, Basel, Switzerland. This article is an open access article distributed under the terms and conditions of the Creative Commons Attribution (CC BY) license (<https://creativecommons.org/licenses/by/4.0/>).

## 1. Introduction

Thousands of compounds have been identified from the mainstream smoke of tobacco so far. These compounds include toxic constituents as well as flavor agents that endow the tobacco products with unique characteristics [1–7]. Precise identification of the compounds in the mainstream smoke is the foundation for understanding the potential influence of tobacco on human health and the design of user-friendly tobacco products. The primary challenge for the analysis of mainstream smoke is the difficulty of collecting the components such as glycerol and glycerol triacetate from the mainstream effectively.

The particulate phase, which is mainly condensed droplets with a size of ~0.2 to 0.4 µm, is the main phase of mainstream smoke [8]. In general, analysis of the particulate phase is conducted by collecting the particulate phase from the mainstream, followed by extraction and quantification of desired components from the collected particulate phase. Materials with rich polar functional groups (e.g., hydroxyl groups) can be used for trapping the mainstream smoke. Cellulose-based material is a class of low-cost and biocompatible material that has a high potential for effective trapping of the particulate phase. However, the use of cellulose-based materials for such applications has not been explored. According to a standard protocol [9], glass fiber pads used as smoke filters are properly fitted into holders and conditioned in a test atmosphere for more than 12 h. Afterwards, smoking experiments are conducted with a smoking machine, and the particulate in the smoke is trapped in the glass fiber pad. The weight difference of the glass fiber pad before and after smoking experiments was recorded and used to analyze the amount of total particulate matter (TPM) [10]. In addition, the substances on the particulate matter can be extracted with 2-propanol and further analyzed. Depending on the upper limit of TPM to be analyzed (150 mg or 600 mg), a glass fiber pad with a diameter 44 mm or 92 mm is used.

The Cambridge filter pad (CFP) is the most commonly used smoke filter. So far, CFP has been widely used to trap TPM for the analysis of substances adsorbed on TPM such as particle state radicals [11], gas phase radicals [12], nicotine [13], aromatic amines [14], benzopyrene [15], aldehyde species [16], and polycyclic aromatic hydrocarbons [17]. Despite the successful use of CFP for the trapping and analysis of tobacco mainstream smoke, the high cost of CFP might limit its widespread use. Herein, we report the development of a low-cost alternative to CFP, which is a tri-layer pad composed of environmentally friendly cellulose-based materials. Such a cellulose-based trapping pad is of low cost. In addition, its preparation is simple and does not require the use of a binder material that could interfere with the trapping process. The trapping behavior of the novel tri-layer pad was quantified and compared with CFP.

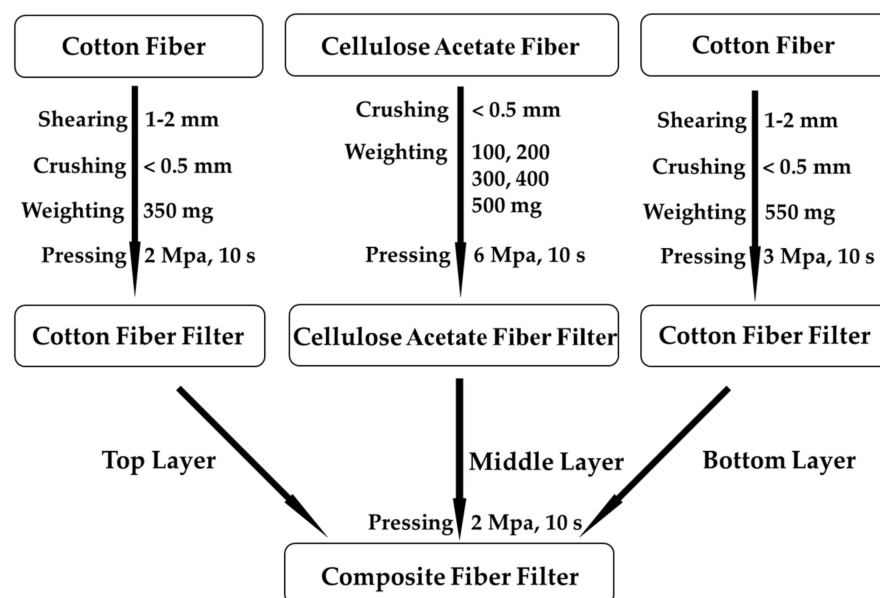
## 2. Materials and Equipment

### 2.1. Materials

Isopropanol (99.7 wt%, Shanghai, China), naphthalene (99.0 wt%, Shanghai, China), glycerol (99.0 wt%, Shanghai, China), glyceryl triacetate (99.0 wt%, Shanghai, China) and Whatman Cambridge filters (Shanghai, China) were purchased from Alladin Reagent Co., Ltd. Cotton fiber was purchased from Tai'an Dayu Textile Co., Ltd. (Taian, China), and cellulose acetate fiber was obtained from HuBei Tobacco Co. Ltd. (Wuhan, China). Nonflammable cigarette products MOK and COO were provided by China Tobacco Hubei Co., Ltd. (Wuhan, China). The length of COO was ~5.5 cm. A high-speed multifunction crusher (800Y, Boou Hardware Products Co., Ltd., Yongkang, China) and tablet press (PC-24S, Pinchuang Technology Co., Ltd., Guilin, China) were used.

### 2.2. Preparation of Composite Fiber Filter

A composite fiber filter was made by pressing three layers of filter, in which the top and bottom layers were cotton fibers with different pore sizes, and the interlayer was a cellulose acetate fiber filter. The production flow chart is shown in Scheme 1.



**Scheme 1.** Schematic diagram of production process for three-layer composite filter.

#### 2.2.1. Preparation of Cotton Fiber Filter

Firstly, the natural cotton fiber filter plate was cut into broken fibers with a growth degree of 1–2 mm, and the broken fibers were further crushed to a length <0.5 mm by a high-speed multi-functional crusher. After the above treated cotton fibers were dispersed, 350 mg was weighed to produce a uniform circular cake with a diameter of 42 mm and a

thickness of 3–5 mm. The pressure of the tablet press was controlled at 2 MPa, which was maintained for 10 s, and the cotton fiber filter was pressed as the top layer of the composite filter. The preparation method for the bottom cotton fiber filter was similar to that of the top layer. The mass of the cotton fiber was 550 mg, the pressure of the tablet press was 3 MPa, the pressure was maintained for 10 s, and the cotton fiber filter was pressed and used as the bottom layer of the composite filter.

#### 2.2.2. Preparation of Cellulose Acetate Fiber Filter

Cellulose acetate fiber samples weighing 100, 200, 300, 400 and 500 mg, respectively, were crushed to a length <0.5 mm with a high-speed multi-functional crusher. The pressure of the tablet press was controlled at 6 Mpa, the pressure was maintained for 10 s, and the cellulose acetate fiber filter with a diameter of 42 mm and uniform thickness was pressed.

#### 2.2.3. Pressing of Three Layers of Filter

The cotton fiber filter plate and cellulose acetate fiber filter plate were placed in sequence and pressed together by the tablet press. The pressure of the tablet press was 2 MPa, and the pressure was maintained for 10 s to prepare the composite fiber filter plate.

#### 2.3. Mainstream Smoke Capture Experiment

The composite filter prepared above and the Cambridge filter pad were put into the filter holder, respectively. Ten blank heated non-burning cigarettes were selected, and the particle phase composition in the mainstream smoke was captured by the self-made smoking device in the laboratory for subsequent quantification. The heating chamber was heated to 250 °C and the release experiment began. The suction interval was 30 s, and the suction duration was 2 s. The suction volume was set to be 55 mL, and a total of 8 aspirations were taken.

#### 2.4. Quantitative Analysis Experiment

The quantitative analysis experiment was similar to that in reference [18]. The composite fiber filter and glass fiber filter with trapped mainstream smoke particulates were respectively put into sample bottles, 20 mL isopropanol solution containing internal standard naphthalene (20 mg/L) was added, and the extraction was conducted at room temperature for 60 min with oscillation. After centrifugation, the supernatant was collected for gas chromatographic analysis.

The GC conditions were the same as those in reference [18]. For accurate quantification, standard solutions of 2 mg L<sup>-1</sup>, 4 mg L<sup>-1</sup>, 6 mg L<sup>-1</sup>, 8 mg L<sup>-1</sup>, and 10 mg L<sup>-1</sup> glycerol and triglyceride triacetate were prepared, and the standard curves were determined.

#### 2.5. Characterizations

**FTIR measurement:** A drop of glycerin or triglyceride triacetate was placed on the surface of cotton fiber, cellulose acetate fiber, and glass fiber, respectively. The FTIR spectra were detected by a VATAR FT-IR370 spectrometer after the sample was dry. The wavelength range was 400–4000 cm<sup>-1</sup>. Sixty-four scans were conducted for each FTIR measurement.

**Scanning electron microscope (SEM) characterization:** A JSM-7500F/JSM-7500F scanning electron microscope was used to photograph the surface morphology of cotton fiber, cellulose acetate fiber, glass fiber, respectively. The accelerating voltage was 10.0 kV. Before testing, the surface of each material was coated with gold by sputtering coater (Hitachi, E-1010, Hitachi International Ltd., Tokyo, Japan).

**XRD (X-ray diffraction):** Cotton fiber filter, cellulose acetate fiber filter, and glass fiber filter were measured with an Empyrean instrument, respectively using Cu K $\alpha$  radiation of wavelength 1.5406 Å (40 kV, 40 mA). The scanning range was 10–50°.

**DFT (density function theory) analysis:** All structural optimizations and energy calculations were performed using Materials Studio's DMol3 module. The generalized gradient approximation (GGA)-Perdew–Burke–Ernzerhof (PBE) functional was used to calculate the

exchange correlation energy. The basis set of double numerical orbits + orbital polarization function (DNP) was selected. In order to accelerate the convergence rate of self-consistent field (SCF) iteration and allow orbit relaxation during calculation, Fermi Smearing was set to 0.005 Ha. The convergence criteria of atomic energy change, maximum stress and displacement were set as  $1 \times 10^{-5}$  Ha,  $2 \times 10^{-3}$  Ha/A, and  $5 \times 10^{-3}$  Å, respectively. After the convergence test, the orbital cutoff accuracy was set to 4.9 Å; the binding energy ( $E_b$ ) calculation formula is as follows:

$$E_b = E_{\text{total}} - E_G - E_C \quad (1)$$

where,  $E_{\text{total}}$ ,  $E_G$ ,  $E_C$  represent the total energy after combination and the monomer energy after structural optimization, respectively.

### 3. Results and Discussion

#### 3.1. Compositional and Morphological Characterizations

A tri-layer pad was designed as a mainstream smoke filter. In the middle of the pad, a cellulose acetate fiber membrane (CAF) with high hydrophobicity was used to trap particulate matter in the mainstream. Hydrophilic cotton fiber (CF) membrane was composited on both sides of the cellulose acetate fiber membrane to construct the composite pad (abbreviated as CF/CAF/CF in the following). The CF layer had a relatively larger pore size than the CAF interlayer and was used to trap water vapor and hydrophilic components in the mainstream. The two surface CF layers were endowed with different porous features for effective filtering of particulate matter of different sizes. The control of the porous properties of the CF layer was realized by the control of pressure during layer fabrication. The compositions of the CF, CAF, and CFP were firstly analyzed with XRD characterizations. As seen in Figure 1, the XRD pattern of CFP showed a broad peak centered at  $\sim 28^\circ$  [19], which is typical for an amorphous  $\text{SiO}_2$  material. CAF also showed a broad peak at  $\sim 20.9^\circ$  [20], which could be probably attributed to the characteristic  $I_\beta$  peak of cellulose material. In comparison, a series of well-developed crystalline peaks of cellulose could be identified from the XRD spectra of CF. These peaks were (101) peak ( $2\theta = 14.8^\circ$ ), ( $10\bar{1}$ ) peak ( $2\theta = 20.60^\circ$ ), (002) peak ( $2\theta = 22.8^\circ$ ) and (040) peak ( $2\theta = 34.5^\circ$ ) [21]. Additionally, according to the formula reported in the literature [22], the crystallinity index of CF was calculated as 32.04%. The morphology of the CFP and CF/CAF/CF filter were investigated with SEM (Figure 2). CFP exhibited a uniform fibrous structure. The fiber diameter ranged from tens to hundreds of nm. Irregular pores formed by the stacking of fibers were present in CFP, and the average pore size was in the scale of tens of  $\mu\text{m}$ . Compared to CFP, the diameters of the CF and CAF fibers were much larger. In addition, the fibers of CF and CAF were stacked compactly. Therefore, their porosity was lower than that of CFP. Such a compact structure might be advantageous for the trapping of mainstream components. The porosity of the top CF layer (Figure 2B) was slightly higher than that of the bottom CF layer (Figure 2D) due to the smaller compression pressure used during layer fabrication.

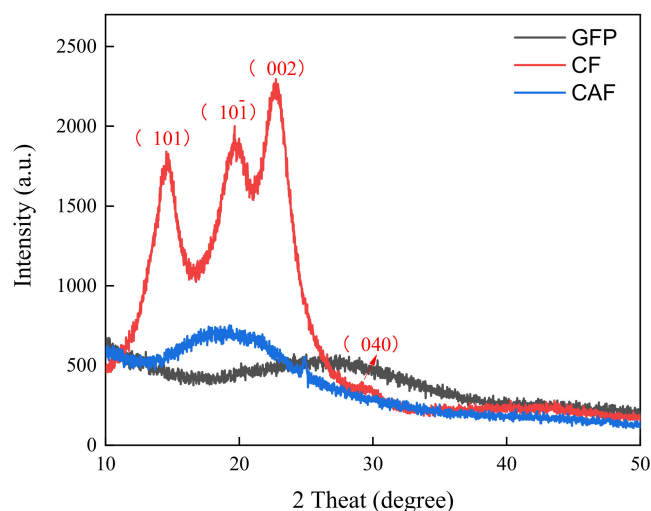


**Figure 1.** XRD patterns of Cambridge filter pad (CFP), cotton fiber layer (CF), and cellulose acetate fiber interlayer (CAF).

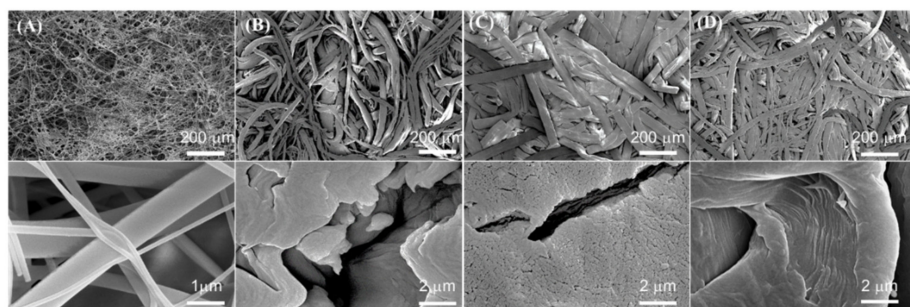


**Figure 2.** SEM images of (A) Cambridge filter pad (CFP), (B) top cotton fiber layer (CF), (C) cellulose acetate fiber interlayer (CAF), and (D) bottom CF layer.

### 3.2. Interactions between the CF/CAF and Glycerol/Glycerol Triacetate

Both CF and CAF have high affinity with typical constituents in the mainstream of tobacco smoke. To demonstrate this point, DFT analysis was conducted. Structural models of  $\text{SiO}_2$ , cellulose, and cellulose acetate, mimicking CFP, CF, and CAF, respectively, were constructed. Glycerol and glycerol triacetate, major additives in cigarette filters, were selected as model substances to evaluate the affinity between the mainstream components and the filter pad. The binding energies of glycerol and glycerol triacetate on  $\text{SiO}_2$  were calculated to be 0.234 and 0.241 eV, respectively (Figure 3). These positive binding energies suggest that adsorption of glycerol and glycerol triacetate on  $\text{SiO}_2$  is thermodynamically unfavorable. In contrast, the binding energies of glycerol and glycerol triacetate on both CAF and CF were negative, suggesting that CAF and CF have higher affinity with mainstream components than  $\text{SiO}_2$ . Such a high affinity is beneficial for the trapping of these components from the smoke mainstream. The binding of glycerol and glycerol triacetate with CFP, CF, and CAF was further characterized in FTIR experiments (Figure 4). The FTIR spectra of glycerol and glycerol triacetate were firstly collected and used as a reference. The FTIR spectra of glycerol showed a characteristic peak for the stretching vibration of OH- bond ( $3290\text{ cm}^{-1}$ ) [23]. Characteristic peaks assigned to stretching vibrations of  $\text{-C=O}$  ( $1740\text{ cm}^{-1}$ ) and  $\text{-C-O-}$  ( $1040\text{ cm}^{-1}$ ) were identified from the spectra of glycerol triacetate [24]. The FTIR spectra of CFP, CF and CAF was also collected. For CFP, a typical band associated with Si-O-Si asymmetric stretching vibration ( $1030\text{ cm}^{-1}$ ) was observed in the FTIR spectra [25]. The FTIR spectra of CF showed a peak for the in-plane wagging vibration of  $\text{-OH}$ . In addition, the peak assigned to the stretching vibration of  $\text{-C=O}$  ( $1740\text{ cm}^{-1}$ ) was present in the spectra. This peak could be originated from the protein and pectin in CF [26].



The peak for the stretching vibration of  $\text{-C=O}$  was also observed in the spectra of CAF because CAF is rich in acetyl groups [27]. The bands corresponding to the stretching vibration of the OH-bond ( $3290\text{ cm}^{-1}$ ), C-H stretching vibration ( $2930\text{ cm}^{-1}$ ,  $2870\text{ cm}^{-1}$ ),  $\text{CH}_2$  symmetric bending vibration ( $1430\text{ cm}^{-1}$ ), C-O stretching of the secondary alcohol ( $1105\text{ cm}^{-1}$ ), and C-O stretching of the primary alcohol ( $1040\text{ cm}^{-1}$ ) were observed in the FTIR spectra of glycerol-loaded samples (glycerin@CFP, glycerin@CF, and glycerin@CAF) [23]. Similarly, bands from glycerol triacetate also occurred in the FTIR spectra of glycerol triacetate@CFP, glycerol triacetate@CF, and glycerol triacetate@CAF ( $2950\text{ cm}^{-1}$  for  $\text{CH}_2$  asymmetrical stretching vibration,  $1740\text{ cm}^{-1}$  for  $\text{C=O}$  stretching vibration,  $1370$ ,  $1220\text{ cm}^{-1}$  C-H deformation vibrations, and  $1040\text{ cm}^{-1}$  for C-O stretching vibration) [24]. These results show that CFP, CF, and CAF could adsorb glycerol and glycerol triacetate and be used as filters for these substances.

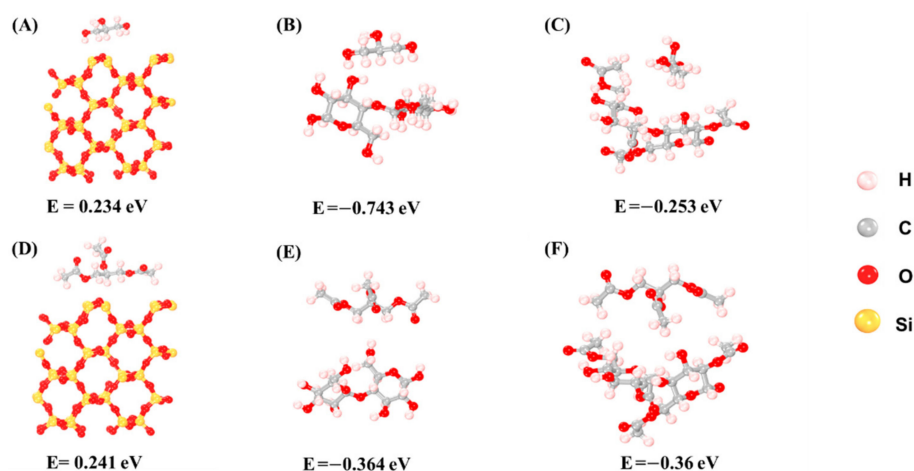


**Figure 3.** Optimized configuration showing the adsorption of glycerol on (A)  $\text{SiO}_2$ , (B) cellulose, and (C) cellulose acetate, and glycerol triacetate on (D)  $\text{SiO}_2$ , (E) cellulose, and (F) cellulose acetate.

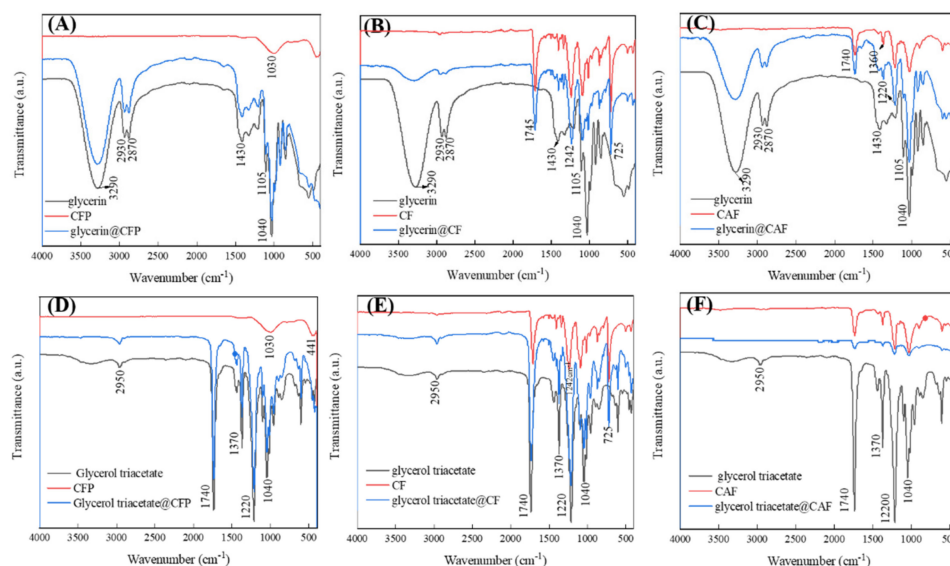


**Figure 4.** FTIR spectra of (A) CFP, (B) CF, and (C) CAF adsorbed with glycerol and (D) CFP, (E) CF, and (F) CAF adsorbed with glycerol triacetate.

### 3.3. Trapping Performance of CF/CAF/CF Pad

Finally, the triglyceride triacetate and glycerol trapping performance of the filter pads was evaluated. The weight of the CAF interlayer varied from 0.1 g to 0.5 g to probe the effect of the CAF interlayer on the trapping performance of the CF/CAF/CF pad. Each experiment was repeated at least three times, and the average value of the trapped

weight is shown (Figure 5, Table S1). CFP showed poor trapping performance against glycerol triacetate. The weight of the collected glycerol triacetate on CFP was 0.03 mg, 0.04 mg, 0.08 mg, 0.18 mg, 0.12 mg, 0.06 mg, 0.08 mg, and 0.07 mg from the 1st suction to the 8th suction, respectively. In the 4th suction, CFP trapped the highest amount of glycerol triacetate. All of the CF/CAF/CF pads showed significantly higher glycerol triacetate collection performance than CFP. For example, the trapped glycerol triacetate on CF/CAF<sub>0.4</sub>/CF was 0.87 mg, 0.64 mg, 0.90 mg, 0.53 mg, 1.01 mg, 0.85 mg, 0.77 mg, and 0.97 mg from the 1st suction to the 8th suction. The total weight of the collected glycerol triacetate on CF/CAF<sub>0.2</sub>/CF reached 4.77 mg, 623% higher than that for CFP. The high amount of glycerol triacetate trapped on CF/CAF/CF could be because the polarity of glycerol triacetate is close to that of cellulose acetate. The glycerol trapping performance of CFP was close to that of the CF/CAF/CF pad. Varying the interlayer weight of CF/CAF/CF did not influence the trapping performance of the CF/CAF/CF pad. Among all of the samples, CF/CAF<sub>0.2</sub>/CF showed the highest trapping capability. The glycerol collected on CF/CAF<sub>0.2</sub>/CF was 0.12 mg, 0.11 mg, 0.18 mg, 0.48 mg, 0.77 mg, 0.72 mg, 0.45 mg, and 0.24 mg from the 1st suction to the 8th suction, respectively. Based on all of the results above, CF/CAF<sub>0.2</sub>/CF is the optimal choice for the fabrication of mainstream smoke filters due to its balanced smoke trapping performance and material cost.

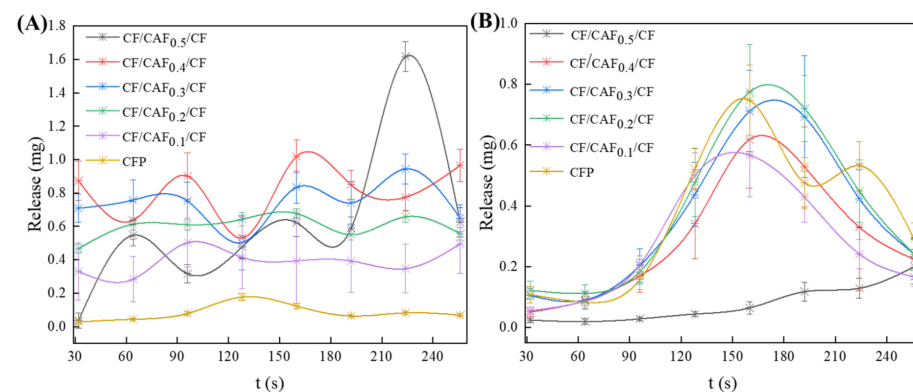


**Figure 5.** Quantified trapping of (A) glycerol triacetate and (B) glycerol with CFP and different CF/CAF/CF pads at different puffs.

#### 4. Conclusions

A three-layer mainstream smoke filter, with cotton fiber (CF) layers on both sides and a cellulose acetate fiber (CAF) interlayer in between, was developed. Both the CF and CAF have high affinity with the constituents of mainstream smoke, such as glycerol and glycerol acetate. Therefore, the composite CF/CAF/CF filter could effectively collect these constituents from the mainstream smoke. A comparative study showed that the as-developed CF/CAF<sub>0.2</sub>/CF filter is superior to the standard CFP filter. We envision that the newly developed CF/CAF/CF filter may find many applications in the analysis of mainstream smoke.

**Supplementary Materials:** The following supporting information can be downloaded at: <https://www.mdpi.com/article/10.3390/app12094196/s1>, Table S1: The weight of detected glycerin and triglyceride triacetate on CF/CAF/CF pad with different interlayer weights and CPF.

**Author Contributions:** Conceptualization, J.L.; methodology, X.D. and X.C.; validation, X.S., M.W. and Y.H.; formal analysis, X.P.; investigation, X.C.; writing—original draft preparation, X.C.; writing—review and editing, J.L.; supervision, M.W., X.D. and J.L.; project administration, J.L.; funding acquisition, J.L. All authors have read and agreed to the published version of the manuscript.

**Funding:** This research was funded by Hubei China Tobacco Industry Co., Ltd., grant number 2021JCXL2JS2A001.

**Institutional Review Board Statement:** Not applicable.

**Informed Consent Statement:** Not applicable.

**Data Availability Statement:** The data presented in this study are available in the current manuscript.

**Conflicts of Interest:** The authors declare no conflict of interest.

## References

1. Wei, M.; Pan, X.; Rong, L.; Dong, A.J.; He, Y.L.; Song, X.Y.; Li, J.S. Polymer carriers for controlled fragrance release. *Mater. Res. Express* **2020**, *7*, 082001. [\[CrossRef\]](#)
2. Wei, M.; Song, X.Y.; Pan, X.; Li, R.; Chen, C.; Du, X.D.; Li, J.S. Thermal Triggered Release of Menthol from Different Carriers: A Comparative Study. *Appl. Sci.* **2020**, *10*, 1677. [\[CrossRef\]](#)
3. Narkowicz, S.; Polkowska, Z.; Kielbratowska, B.; Namiesnik, J. Environmental Tobacco Smoke: Exposure, Health Effects, and Analysis. *Crit. Rev. Environ. Sci. Technol.* **2013**, *43*, 121–161. [\[CrossRef\]](#)
4. Borgerding, M.; Klus, H. Analysis of complex mixtures—Cigarette smoke. *Exp. Toxicol. Pathol.* **2005**, *57*, 43–73. [\[CrossRef\]](#) [\[PubMed\]](#)
5. Smith, C.J.; Livingston, S.D.; Doolittle, D.J. An international literature survey of “IARC Group I carcinogens” reported in mainstream cigarette smoke. *Food Chem. Toxicol.* **1997**, *35*, 1107–1130. [\[CrossRef\]](#)
6. Soleimani, F.; Dobaradaran, S.; De-la-Torre, G.E.; Schmidt, T.C.; Saeedi, R. Content of toxic components of cigarette, cigarette smoke vs cigarette butts: A comprehensive systematic review. *Sci. Total Environ.* **2022**, *813*, 152667. [\[CrossRef\]](#)
7. Schick, S.; Glantz, S. Philip Morris toxicological experiments with fresh sidestream smoke: More toxic than mainstream smoke. *Tob. Control* **2005**, *14*, 396–404. [\[CrossRef\]](#)
8. Brokl, M.; Bishop, L.; Wright, C.G.; Liu, C.; McAdam, K.; Focant, J.F. Analysis of mainstream tobacco smoke particulate phase using comprehensive two-dimensional gas chromatography time-of-flight mass spectrometry. *J. Sep. Sci.* **2013**, *36*, 1037–1044. [\[CrossRef\]](#)
9. *Cigarettes-Determination of Total and Nicotine-Free Dry Particulate Matter Using a Routine Analytical Smoking Machine*; International Organization for Standardization: Geneva, Switzerland, 2019; p. 19.
10. Hasan, F.; Khachatryan, L.; Lomnicki, S. Comparative Studies of Environmentally Persistent Free Radicals on Total Particulate Matter Collected from Electronic and Tobacco Cigarettes. *Environ. Sci. Technol.* **2020**, *54*, 5710–5718. [\[CrossRef\]](#)
11. Zhou, J.; Wu, K.; Sun, Y.; Cong, J.-B.; Wang, C.-Z.; Chang, X.; Xian, H.; Zhu, Y.-F. A novel method for quantitative analysis of total particulate-phase free radicals in mainstream cigarette smoke. *Acta Chim. Sin.* **2008**, *66*, 216–222.
12. Wooten, J.B. Gas-Phase Radicals in Cigarette Smoke: A Re-evaluation of the Steady-State Model and the Cambridge Filter Pad. *Mini-Rev. Org. Chem.* **2011**, *8*, 412–426. [\[CrossRef\]](#)
13. Zuccarello, P.; Rust, S.; Caruso, M.; Emma, R.; Pulvirenti, R.; Favara, C.; Polosa, R.; Li Volti, G.; Ferrante, M. Nicotine dosimetry and stability in cambridge filter PADs (CFPs) following different smoking regime protocols and storage conditions. *Regul. Toxicol. Pharmacol.* **2021**, *122*, 104917. [\[CrossRef\]](#) [\[PubMed\]](#)
14. Xie, F.; Yu, J.; Wang, S.; Zhao, G.; Xia, Q.; Zhang, X.; Zhang, S. Rapid and simultaneous analysis of ten aromatic amines in mainstream cigarette smoke by liquid chromatography/electrospray ionization tandem mass spectrometry under ISO and “Health Canada intensive” machine smoking regimens. *Talanta* **2013**, *115*, 435–441. [\[CrossRef\]](#) [\[PubMed\]](#)
15. Ding, Y.S.; Chou, T.; Abdul-Salaam, S.; Hearn, B.; Watson, C.H. Development of a Method to Estimate Mouth-Level Benzo a pyrene Intake by Filter Analysis. *Cancer Epidemiol. Biomark. Prev.* **2012**, *21*, 39–44. [\[CrossRef\]](#) [\[PubMed\]](#)
16. Pauwels, C.G.G.M.; Klerx, W.N.M.; Pennings, J.L.A.; Boots, A.W.; van Schooten, F.J.; Opperhuizen, A.; Talhout, R. Cigarette Filter Ventilation and Smoking Protocol Influence Aldehyde Smoke Yields. *Chem. Res. Toxicol.* **2018**, *31*, 462–471. [\[CrossRef\]](#)
17. Ding, Y.S.; Trommel, J.S.; Yan, X.Z.J.; Ashley, D.; Watson, C.H. Determination of 14 polycyclic aromatic hydrocarbons in mainstream smoke from domestic cigarettes. *Environ. Sci. Technol.* **2005**, *39*, 471–478. [\[CrossRef\]](#)
18. Song, X.; Wei, M.; Pan, X.; He, Y.; Cui, X.; Du, X.; Li, J. Heat Triggered Release Behavior of Eugenol from Tobacco Leaf. *Appl. Sci.* **2021**, *11*, 8642. [\[CrossRef\]](#)
19. Deshmukh, P.; Bhatt, J.; Peshwe, D.; Pathak, S. Determination of silica activity index and XRD, SEM and EDS studies of amorphous SiO<sub>2</sub> extracted from rice husk ash. *Trans. Indian Inst. Met.* **2011**, *65*, 63–70. [\[CrossRef\]](#)
20. Wang, L.; Xu, Y.; Li, Z.; Wang, H.; Zhang, Q.; Pang, J. Preparation and Characterization of Cellulose Acetate/Chitosan Composite Film with High Mechanical Strength. *Chem. Ind. For. Prod.* **2020**, *40*, 107–113. [\[CrossRef\]](#)
21. Liu, Z.; Gao, Y.; Jin, H.; Yu, S. Study on natural cellulose crystallinity determined by the technology of XRD peak separation. *China Meas. Test* **2015**, *41*, 38–41. [\[CrossRef\]](#)
22. Ruangudomsakul, W.; Ruksakulpiwat, C.; Ruksakulpiwat, Y. Preparation and Characterization of Cellulose Nanofibers from Cassava Pulp. *Macromol. Symp.* **2015**, *354*, 170–176. [\[CrossRef\]](#)
23. Maquirriain, M.A.; Neyertz, C.A.; Querini, C.A.; Pisarello, M.L. Crude glycerine purification by solvent extraction. *Braz. J. Chem. Eng.* **2021**, *39*, 235–249. [\[CrossRef\]](#)
24. Zięba, A.; Pacuła, A.; Drelinkiewicz, A. Transesterification of triglycerides with methanol catalyzed by heterogeneous zinc hydroxy nitrate catalyst. Evaluation of variables affecting the activity and stability of catalyst. *Energy Fuels* **2010**, *24*, 634–645. [\[CrossRef\]](#)



- 
25. Samoedro, B.; Irmansyah; Irzaman. SEM, EDX, and FTIR analysis from Salak Pondoh skin extracted SiO<sub>2</sub>. *AIP Conf. Proc.* **2021**, *2320*, 030004.
  26. Zhang, L.; Zhang, S.; Xu, P.; Li, X. Study Crystallinity of the Developing Cotton Fibers by Micro-Fourier Transform Infrared Spectroscopy (FTIR) and X-ray Diffraction (XRD). *Cotton Sci.* **2020**, *32*, 370–380. [[CrossRef](#)]
  27. Ghorani, B.; Kadhodae, R.; Rajabzadeh, G.; Tucker, N. Assembly of odour adsorbent nanofilters by incorporating cyclodextrin molecules into electrospun cellulose acetate webs. *React. Funct. Polym.* **2019**, *134*, 121–132. [[CrossRef](#)]